Energieforschungsprogramm

Publizierbarer Endbericht

Programmsteuerung:
Klima- und Energiefonds (KLIEN) und Bundesministerium für Klimaschutz, Umwelt, Energie, Mobilität, Innovation und Technologie (BMK)

Programmabwicklung:
Österreichische Forschungsförderungsgesellschaft mbH (FFG)

Endbericht
erstellt am

20.08.2026

Projekttitel:MAGNIFICO

Development of a protective inorganic interface for using metallic Mg anodes in next-generation Mg-ion batteries (Entwicklung eines anorganischen Interface für die Nutzung metallischen Magnesiums in Mg-Ionen- Batterien der nächsten Generation)

Projektnummer:FO999899395

Ausschreibung	8. Ausschreibung Energieforschungsprogramm
Projektstart	01.01.2023
Projektende	31.12.2025
Gesamtprojektdauer (in Monaten)	36 Monate
ProjektnehmerIn (Institution)	AIT Austrian Institute of Technology GmbH
AnsprechpartnerIn	Dr. Irshad MOHAMMAD
Postadresse	Giefinggasse 2, 1210 Wien
Telefon	050550
Fax	n.a.
E-mail	Irshad.mohammad@ait.ac.at
Website	MAGNIFICO Development of a protective inorganic interface for using metallic Mg anodes - AIT Austrian Institute Of Technology

MAGNIFICO

Development of a protective inorganic interface for using metallic Mg anodes in next-generation Mg-ion batteries (Entwicklung eines anorganischen Interface für die Nutzung metallischen Magnesiums in Mg-Ionen- Batterien der nächsten Generation)

AutorInnen:
Dr. Irshad MOHAMMAD (AIT)
Dr. Jialu CHEN (ISTA)

1 Inhaltsverzeichnis

2 Einleitung

(Deutsche Kurzfassung)

Ziel des MAGNIFICO-Projekts war die Entwicklung von Hochspannungs-Magnesium-Ionen-Batterien unter Verwendung einer Anode auf Basis von künstlich beschichtetem Magnesium(Mg)-Pulver, einer Kathode aus $MgMn_2O_4$, welches nur geringe Mengen an kritischen Rohstoffen enthält, sowie eines herkömmlichen $Mg(TFSI)_2$-Elektrolyten.

In diesem Zusammenhang wurde ein sicherer, skalierbarer und nachhaltiger zweistufiger nasschemischer Prozess etabliert, um Schutzschichten auf Basis von Wismut, Zinn oder Indium (Bi, Sn, In) auf Magnesiummetallpulverpartikeln zu synthetisieren.

Im ersten Schritt wurde ein Ätzverfahren für Mg-Pulver entwickelt, bei dem die native Oxidschicht mit einer umweltfreundlichen organischen Säure, Methansulfonsäure (MSA), in Dimethoxymethan (DME) entfernt wird. Im zweiten Schritt wird das geätzte Magnesiumpulver zur Beschichtung der Mg-Pulverpartikel in eine Bi/Sn/In-Chlorid-Lösung in DME überführt.

Das geätzte Mg-Pulver wurde mittels XRD, XRF, XPS und SEM-EDX charakterisiert. Anschließend wurde eine Elektrode auf Basis des geätzten Mg-Pulvers unter Verwendung traditioneller Methoden, einschließlich eines Slurry- und Elektrodenbeschichtungsprozesses, hergestellt. Wir testeten die Leistung der Elektroden aus geätztem Mg-Pulver in symmetrischen und Vollzellenkonfigurationen unter Verwendung eines 0,4 M APC $(PhMgCl)_2$-$AlCl_3$/THF-Elektrolyten. In einer symmetrischen Zelle blieb die geätzte Mg-Pulver-Elektrode über 1000 Lade-/Entladezyklen bei Stromdichten von 0,1 und 1 mA cm−2 stabil.

Die Mg-Pulver/APC/Mo6S8-Vollzelle erreichte eine hohe Kapazität von etwa 70 mAh g−1 bei einer Coulomb-Effizienz von fast 98 %, die über 2000 Zyklen bei 1C aufrechterhalten wurde. Sie zeigte zudem eine hervorragende C-Raten-Leistung und lieferte 50 mAh g−1 bei 10 C. Die Anwendung der geätzten Magnesiumpulver-Anode wurde erstmals auch in einer Pouchzellkonfiguration unter Verwendung eines APC-basierten Elektrolyten und einer Chevrelphasenkathode (Mo6S8) demonstriert.

Bei ersten Versuchen zur Synthese des beschichteten Mg-Pulvers schlug die Bi-basierte Beschichtung auf den Mg-Partikeln fehl. Es gelang jedoch, sowohl Sn- als auch In-basierte beschichtete Mg-Partikel herzustellen und zu charakterisieren. Diese Schutzbeschichtung verhindert die Zersetzung des $Mg(TFSI)_2$-Elektrolyten und unterdrückt die Oberflächenpassivierung von Magnesium, während sie gleichzeitig eine effiziente Mg^{2+}-Ionendiffusion ermöglicht. Sn-beschichtetes Mg-Pulver wurde für die weitergehende Charakterisierung einschließlich Elektrodenherstellung und Zelltests ausgewählt. Analysen mittels XRD, XPS und Querschnitt-SEM/EDX zeigen, dass die etwa 2 µm dicke Beschichtung gleichmäßig ist und hauptsächlich aus Sn- und Mg_2Sn-Verbindungen besteht. Die Elektrodenherstellung aus Sn-beschichtetem Mg-Pulver erfolgte unter Verwendung von Polyisobutylen als Bindemittel und Toluol als Lösungsmittel. Die oberflächengeschützte Elektrode auf Mg-Basis wurde in symmetrischer Zellenkonfiguration in einem 0,3 M $Mg(TFSI)_2$/DME + Diglyme-Elektrolyten getestet, was dank der Mg-ionenleitenden Eigenschaft der Schutzschicht zu einer stabilen, reversiblen Abscheidung (Plating und Stripping) führte. Die Abscheidung und das Ablösen blieben in $Mg(TFSI)_2$ über 1 200 Zyklen bei 0,01 mA cm^(−2) stabil. Die elektrochemische Impedanzanalyse der geschützten Mg-Elektrode ergab einen Grenzflächenwiderstand von etwa 5 kΩ, der fast 19-mal höher war als der von reinem Mg-Pulver in einem 0,3 M $Mg(TFSI)_2$/DME + Diglyme-Elektrolyten, was das Vorhandensein einer Schnelldiffusionsschicht auf der Mg-Oberfläche bestätigte. Was die Tests mit der Sn-beschichteten Elektrode in der Vollzelle betrifft, so wurde diese zunächst mit $MgMn_2O_4$-Material als Kathode kombiniert, das im Arbeitspaket (WP) 6 synthetisiert wurde. Da die Zelle mit der $MgMn_2O_4$-Kathode jedoch nicht ordnungsgemäß funktionierte, entschieden wir uns, für die Vollzellentests in $Mg(TFSI)_2$-Elektrolyt eine Chevrelphasenkathode zu verwenden. Diese Zelle zeigte eine gute Leistung und erreichte über 30 Zyklen bei C/20 eine Kapazität von etwa 80 mAh/g. In dieser Studie zeigt das durch Beschichtung geschützte Mg eine reversible Mg-Plating- und -Stripping-Chemie in einem klassischen etherbasierten Elektrolyten, was die Kompatibilität mit Hochspannungskathoden in Mg-Batterien ermöglicht.

Im Zuge von MAGNIFICO wurden computergestützte Untersuchungen zur strukturellen Stabilität von Sn-, Bi-Phasen und deren Mg-Legierungen unter Verwendung der Dichtefunktionaltheorie (DFT) und des Machine-Learning-Potentials (MLP) durchgeführt. Wir testeten drei Austausch Korrelationsfunktionale (PBE, PBEsol, SCAN) zur Optimierung von Mg-, Sn- und Bi-Metallen sowie bekannter stabiler Legierungen aus Mg-Sn und Mg-Bi. Nach der Berechnung der Kristallgitter und der Bildungsenergien wählten wir PBEsol mit einer 0,02-K-Punkt-Gitterauflösung und einer Cutoff-Energie von 500 eV. Die Berechnungen bestätigen, dass die Mg_2Sn-Phase ($Fm\bar{3}m$) die stabilste Struktur unter den Mg–Sn-Legierungen ist, was mit den experimentellen Ergebnissen übereinstimmt. Zur Unterstützung der rechnerischen Untersuchungen wurden Mg_2Sn- und Bi_2Mg_3-Phasen durch mechanisches Kugelmahlen mit geeigneten Mengen an Mg- und Sn- bzw. Bi-Metallvorläufern synthetisiert. Diese Legierungsphasen wurden mittels XRD-Analyse charakterisiert. Zur Unterstützung der experimentellen Phasenidentifizierung

wurden simulierte XRD-Muster generiert, und die elektronische Leitfähigkeit wurde als Funktion der Ladungsträgerkonzentration analysiert. Zusätzlich wurden Molekulardynamik-Simulationen (unter Verwendung von LAMMPS) und Struktur-Sampling-Techniken eingesetzt, um mögliche Mg–Sn-Konfigurationen zu untersuchen. Es wurde ein Datensatz repräsentativer Strukturen erstellt und mithilfe von DFT-Berechnungen weiter verfeinert, um die Materialcharakterisierung und -modellierung zu unterstützen.
Zuerst wurde ein etablierter Ansatz am damaligen Stand der Technik verwendet, um MLPs für die Mg-Sn- und MgBi-Systeme anzupassen: Nach Erhalt der MgSn- und MgBi-Datensätze nutzten wir das DeepMD-Kit-Paket, um für jedes System ein maßgeschneidertes Machine-Learning-Potential (MLP) anzupassen. In der Mitte des Projekts stellte sich jedoch heraus, dass dieser Ansatz bereits wieder überholt war. Zu den Einschränkungen zählten unzureichende Genauigkeit (nur Drei-Körper-Wechselwirkungen), fehlende Weithaltswechselwirkungen und die Notwendigkeit systemspezifischer („maßgeschneiderter“) Modelle. Um dem entgegenzuwirken, haben wir neuere Methoden angewandt: Fern-MLPs unter Verwendung der Latent Ewald Summation (LES), die die Genauigkeit und Übertragbarkeit verbessern, sowie universelle MLPs, die ohne spezielles Training für viele Materialien funktionieren. Darüber hinaus wurde anstelle der traditionellen Molekulardynamik zur Untersuchung des Phasenverhaltens ein neuer generativer Modellierungsansatz auf Basis von Flow Matching entwickelt. Diese Methode erfasst den Phasenraum (einschließlich diskreter Variablen wie Atomtypen) effizient und kann das Materialverhalten über verschiedene Temperaturen hinweg mit geringerem Rechenaufwand und besserer Skalierbarkeit vorhersagen. Diese neue Methode sowie Validierungen wurden in einem begutachteten Fachjournalartikel veröffentlicht: https://doi.org/10.1021/acs.jctc.5c01248

In Summe wurde im Rahmen des MAGNIFICO-Projekts erfolgreich ein skalierbares nasschemisches Verfahren zum Schutz von Mg-Pulveranoden mit gleichmäßigen Beschichtungen auf Sn-Basis entwickelt, das eine stabile und reversible Mg-Abscheidung in herkömmlichen $Mg(TFSI)_2$-Elektrolyten ermöglicht. Dieser Schutz unterdrückte die Passivierung und die Elektrolytzersetzung bei gleichzeitiger Aufrechterhaltung einer effizienten Mg^{2+}-Diffusion, was bei Vollzellen zu hoher Kapazität (≈70–80 mAh g^{-1}) führte. Darüber hinaus weisen Vollzellen auf Basis von geätzten Mg-Pulverelektroden eine hohe Kapazität und überlegene Hochstromfähigkeit auf und wurden erstmals im Pouch-Cell-Format unter Verwendung eines APC-Elektrolyten demonstriert. Ergänzende DFT-Berechnungen, Legierungssynthese und neueste Ansätze im machine learning (einschließlich Ansätzen zur Langreichweiten- und generativen Flussanpassung) lieferten tiefere Einblicke in die Phasenstabilität und beschleunigten die Materialentwicklung.
Diese Ergebnisse ebnen den Weg für sicherere, nachhaltigere und kostengünstigere Hochspannungs-Magnesium-Ionen-Batterien, die den Einsatz kritischer Rohstoffe minimieren und einen gangbaren Weg zu Energiespeichern der nächsten Generation mit verbesserter Energiedichte, Zyklenlebensdauer und Umweltvorteilen für großtechnische Anwendungen bieten.

(English synopsis)

MAGNIFICO developed high-voltage magnesium-ion batteries utilising an artificially protected magnesium (Mg) powder-based anode, a low-critical-raw-material $MgMn_2O_4$ cathode, and a conventional $Mg(TFSI)_2$ electrolyte. With the help of cutting- edge DFT simulation, safe, scalable and sustainable two-step wet-chemical process was established to synthesise bismuth, tin or indium (Bi, Sn, In) based protective layers on magnesium metal powder particles.

3 Inhaltliche Darstellung

The goal of the MAGNIFICO project was to develop high-voltage magnesium-ion batteries utilising an artificially protected magnesium (Mg) powder-based anode, a low-critical-raw-material $MgMn_2O_4$ cathode, and a conventional $Mg(TFSI)_2$ electrolyte.

Etching Process of Mg powder:

In this project, a safe, scalable, and sustainable etching process was established to etch Mg powder using the environmentally friendly organic acid, methanesulfonic acid (MSA). The etching process in the this project developed to remove the native oxide layer from Mg particle surface. In the etching process, the magnesium powder was stirred in 0.1M MSA/methoxymethane (DME) solution for several hours at room temperature under an inert atmosphere. Figure 1 shows the etching process using Mg powder and foil in a 0.1 M MSA/DME solution. The difference between the start and after 6 hours of etching is clearly visible. Specifically, the Mg foil changed from black to silver, indicating successful etching at 0.1 M concentration of the MSA solution. Additionally, the etched Mg powder looks slightly shinier than the bare Mg powder.

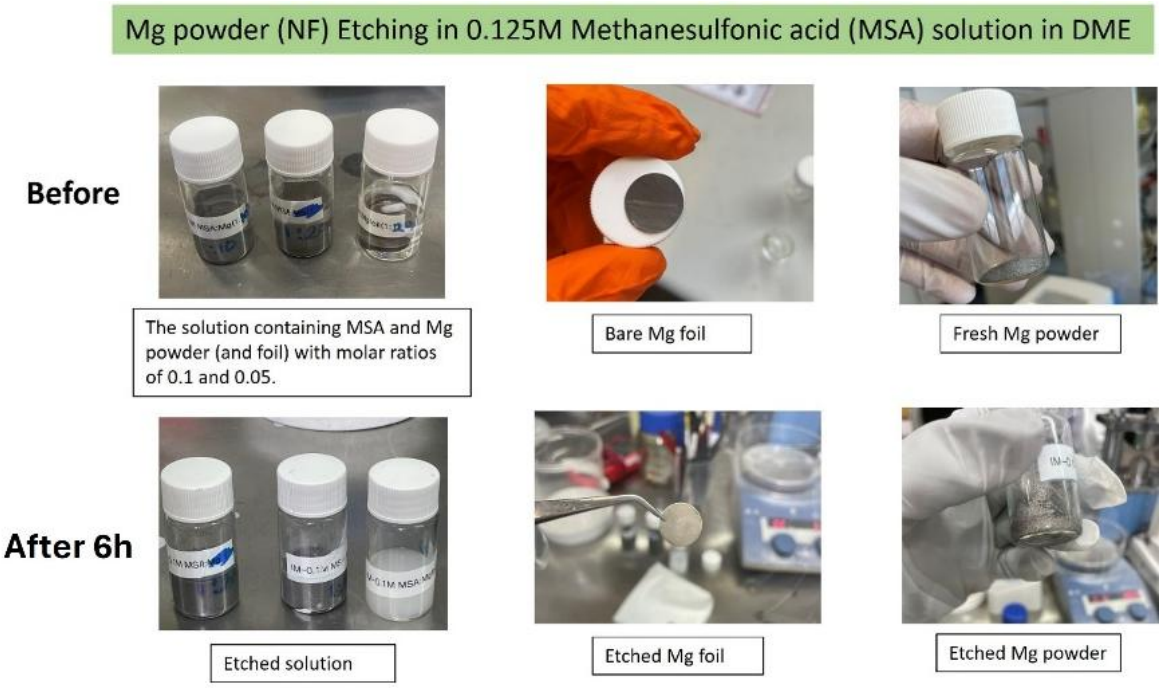

Figure 1. Etching Mg foil and powder in 0.1M MSA/DME solution.

Etched Mg powder was characterised by means of XRD, XRF, XPS, and SEM-EDX, which concludes that methanesulfonic acid etching process of magnesium powder successfully removes $MgCO_3$, MgO, and SiC from its surface.

Mg Electrode Fabrication:

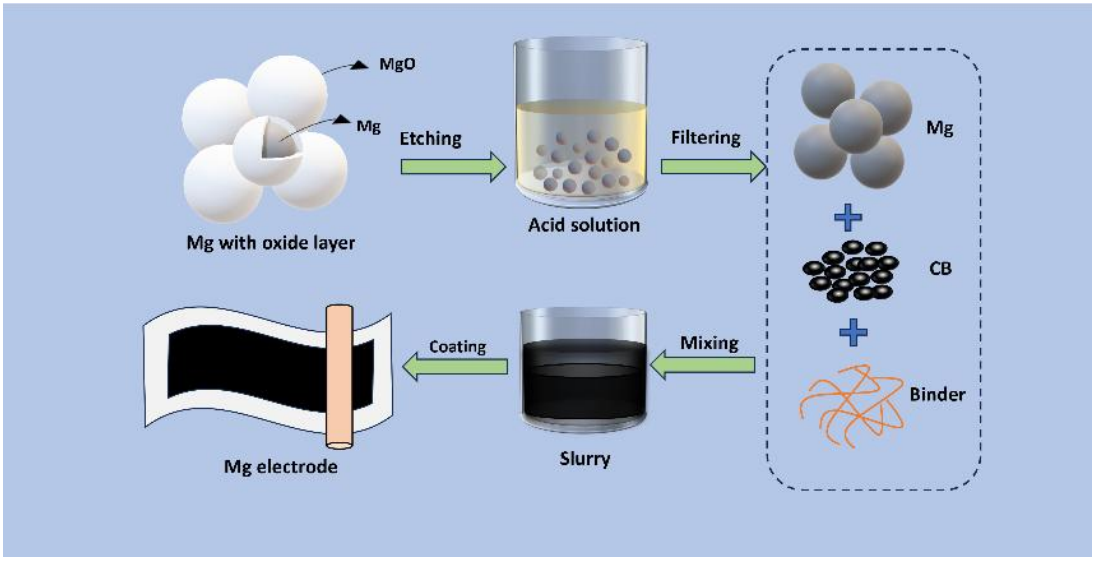

Figure 2. Schematic illustration of etching and electrode fabrication process for Mg powder-based electrodes

The schematic for electrode fabrication from etched Mg powder is shown in Figure 2. The electrode fabrication process for etched Mg powder was quite challenging, and multiple attempts were made to develop Mg powder-based electrodes. All electrode fabrication steps were carried out in an Ar-filled glove box (H_2O and O_2 < 0.1 ppm). Firstly, we attempted to use toluene with an SBR binder, but the SBR binder failed to hold the carbon and magnesium particles together, thereby preventing coating. However, using PVDF binder and DMF solvent allowed us to create a homogeneous slurry, which was successfully casted on Cu and SS current collectors using a doctor blade with a coating gap of 120 µm. After coating, the electrode sheet was left in the glove box for several hours to evaporate the DMF solvent, followed by drying overnight under vacuum at 120 °C to remove residual solvents. Pictures of the PVDF-based coated electrodes are shown in Figure 3a-b. As seen in the images, the Mg electrodes appear compact and homogeneous, with a uniform distribution of all components. Mechanical stability and flexibility of the electrode can be seen in Figure 3b, where an electrode disc was bent without any observed delamination.

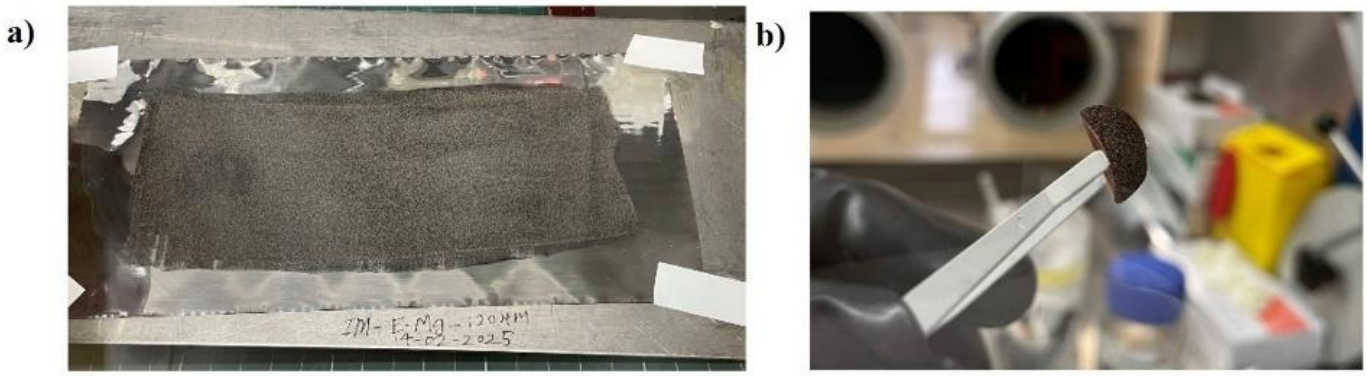

Figure 3.Pictures of an etched Mg electrode on SS current collector using PVDF binder and DMF solvent. (b) Picture of a bent 15mm diameter Mg electrode disc.

Electrochemical Testing of Mg electrode:

We tested the performance of the etched Mg powder electrodes in symmetrical and full-cell configurations using a 0.4 M APC (all phenyl complex) electrolyte in THF (tetra hydro furan). The striping and plating behaviour of Mg symmetrical cells is shown in Figure 4a. In each cycle plating or striping was done for 30 minutes at a constant current density of 0.1 and 1.0 mA/cm^2. A very stable cycling was obtained for etched Mg cells with low overpotentials of around 0.1 and 0.4 V for the current density of 0.1 and 1.0 mA/cm2, respectively. The symmetrical cell based on the etched Mg powder electrode remained stable over 1000 plating/ striping cycles. In comparison to Mg foil, the etched Mg electrode showed superior performance. The improved performance of the etched Mg powder anode can be understood from two complementary effects. First, the etching process removes/reduces the native surface oxide layer and exposes more electrochemically active Mg sites, thereby facilitating Mg dissolution and reducing the interfacial kinetic barrier. Second, the substantially increased specific surface area provides a larger effective electrochemically active area for Mg stripping/plating.

To investigate the enhanced electrochemical performance of the etched Mg electrode, Electrochemical impedance spectroscopy (EIS) analysis was performed on all Mg symmetric cells at open circuit voltage conditions. Figure 4b shows Nyquist plots of symmetric Mg/Mg cells with different Mg electrodes (Mg foil and etched Mg), along with an equivalent circuit used to fit the spectra. As can already be seen from the EIS spectra, the Mg foil-based cell shows high charge transfer resistance of 154 kΩ, whereas the etched Mg-powder electrode yielded a total resistance of approximately 14 kΩ, which is nearly 11-fold lower than that of the Mg foil, suggesting that the etching process enhances interfacial kinetics. Compared with Mg foil, the etched Mg powder electrode showed lower charge-transfer resistances due to its high surface area, arising from the spherical shape of the etched Mg powder, and use of few carbon additive in the Mg electrode formulation.

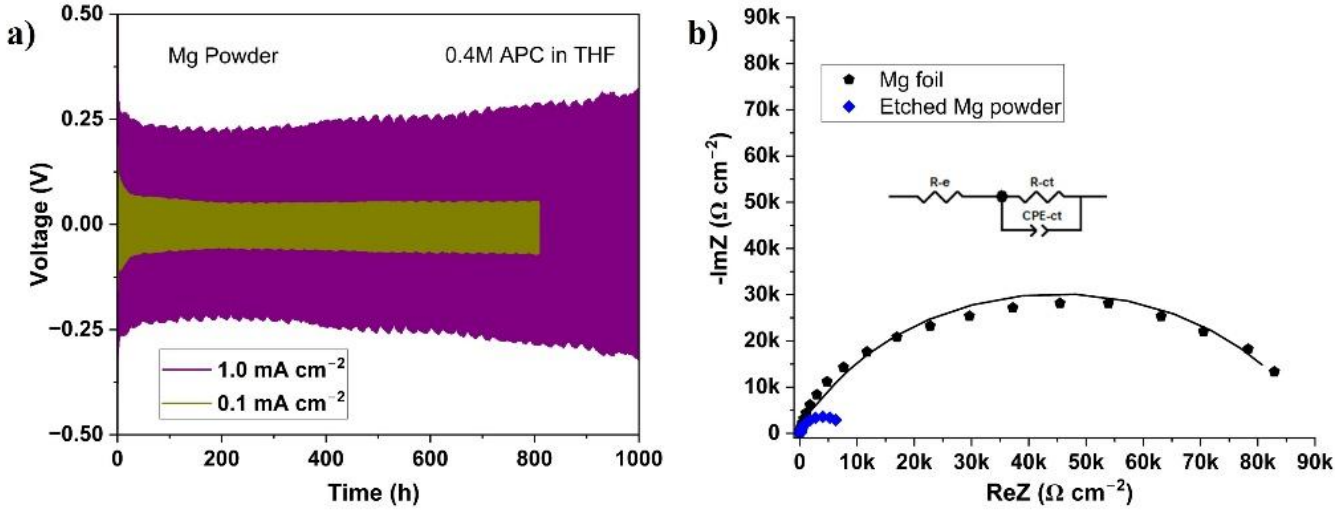

Figure 4. (a) Plating and stripping of Mg powder-based symmetrical cells during long cycling at a current density of 0.1 mA cm^{-2} and 1.0 mA cm^{-2}. (b) Nyquist plots obtained at 25 °C for Mg foil and bare etched Mg powder based symmetrical cells at OCV.

To demonstrate the practical application of the etched Mg anode, full cells were assembled using the Chevrel phase cathode, with APC-based electrolyte. The first five charge-discharge curves of the etched Mg powder/APC/Mo_6S_8 cell in coin format are shown in Figure 5a. As seen there, each cycle exhibited a similar voltage profile with two charge and discharge plateaus, typical of Chevrel phase cathodes. The initial discharge capacity was nearly 75 mAh g^{-1} (5th cycle), which is similar to previous reports, indicating good performance of the etched Mg powder-based cell. Most importantly, the coulombic efficiency for the etched Mg powder-based cell was around 95%, which is quite good for the Chevrel phase cathode. Furthermore, the etched Mg powder-based cell showed high-capacity retention over extended cycling, consistently delivering around 70 mAh g^{-1} after 1000 cycles at 1C, as shown in Figure 5b.

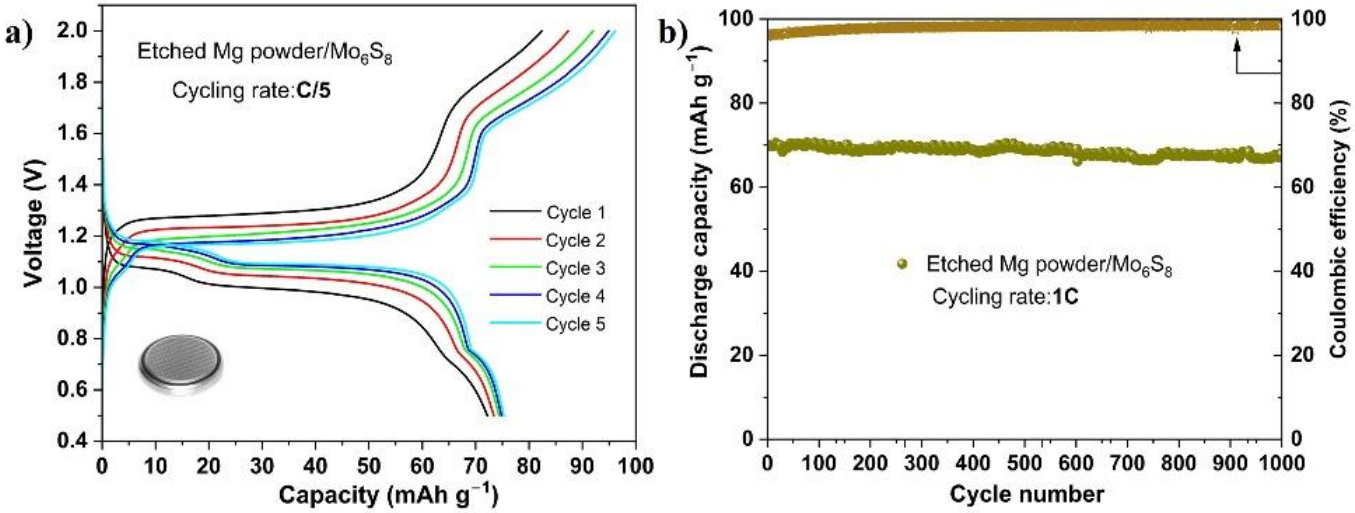

Figure 5 (a). Charge-discharge profiles and (b) cyclic performance of etched Mg powder/APC/Mo_6S_8 cells.

Synthesis of $MgMn_2O_4$

$MgMn_2O_4$ was synthesized using two different methods: the sol–gel (Pechini) method and the alcohol reduction method. In the sol–gel synthesis, magnesium and manganese nitrates were dissolved with citric acid and ethylene glycol in water at appropriate molar ratios, followed by evaporation at approximately 80 °C to form a gel. The gel was subsequently dried at 200 °C for 12 h, ground, and calcined at 400 °C for 10 h to obtain the $MgMn_2O_4$ powder. In the alcohol reduction method, tetrabutylammonium permanganate (n-Bu_4NMnO_4) was first prepared by reacting aqueous tetrabutylammonium bromide with potassium permanganate, followed by filtration, washing, and drying. The synthesized n-Bu_4NMnO_4 was then dispersed in an ethanolic $MgCl_2$ solution to form a colloidal mixture, after which deionized water was added to precipitate $MgMn_2O_4$ (MMO). The resulting precipitate was collected by filtration, washed with water and ethanol, and dried under vacuum at 120 °C overnight.

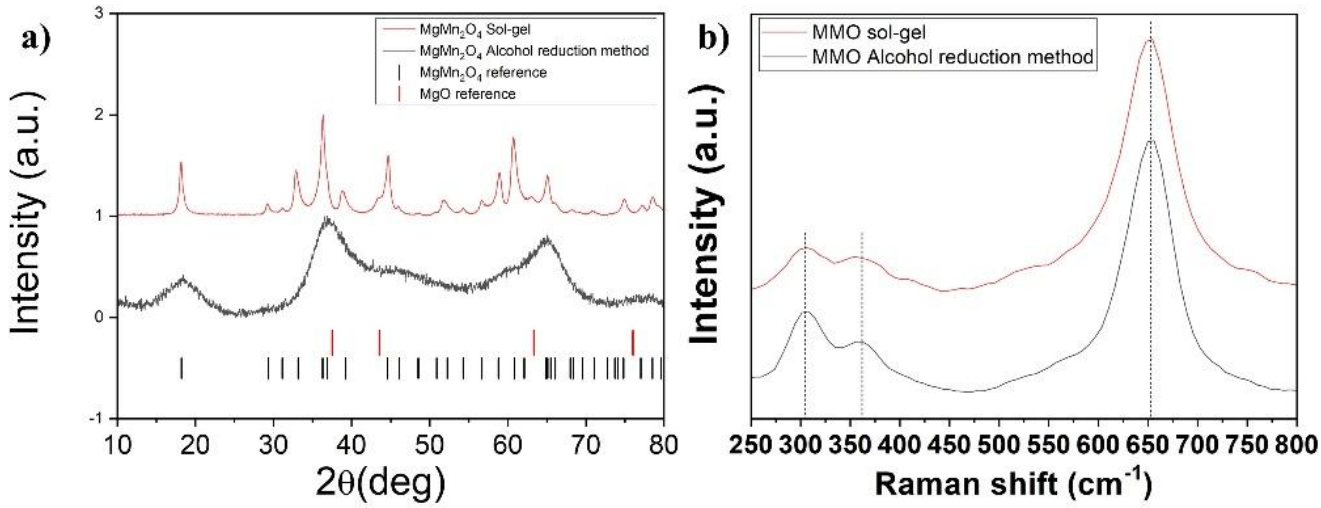

Figure 6. (a) XRD patterns and (b)Raman spectra of MMO synthesized by sol-gel (red) and alcohol reduction method (black)

The XRD patterns and Raman spectra of the MMO synthesized via two different routes is shown in Figure 6. The sol-gel synthesis with a thermal treatment at 400°C produces a crystalline sample. Whereas XRD pattern of MMO synthesize via alcohol reduction method instead shows three main broad peaks, indication that this synthesis route produces a nanocrystalline material. The Raman spectra of MMO is characterized by a strong peak at 653 cm−1 and two less intense bands at 305 and 360 cm−1. The most intense peak at 653 cm−1 can be ascribed to vibrations involving the motion of oxygen atoms inside the MnO6 octahedral units, specifically to the A1g mode (Mn-O stretching vibration). No major differences are observed between the two-synthesis method.

Electrochemical characterization of $MgMn_2O_4$

For electrochemical analysis, $MgMn_2O_4$ based slurry and electrode fabrication was carried out to via NMP based processing. A 15 mm diameter disc of MMO electrode was cycled in coin cell format against activated carbon (AC) in both $Mg(ClO_4)_2$, (b) Mg $(TFSI)_2$ electrolytes. During initial cell testing, it was found

that MMO synthesised via the alcohol reduction method did not perform well. Then, the testing was proceeded with MMO, which was synthesised via the sol-gel route. Figure 7a shows charge-discharge profiles of the MMO cathode versus activated carbon cycled in $Mg(ClO_4)_2$ electrolyte salt at a gravimetric current of 10 mA/g. As it can be seen from the profiles, MMO delivers an initial capacity of 50 mAh/g. The capacity decreases over cycling reaching 20 mAh/g after 100 cycles. This capacity decrease might be due to Mn dissolution into the electrolyte. The potential profile highlights the significant overpotential during charge and discharge, attributed to the (de-) magnesiation of the MMO cathode material.

In the figure 7b, the MMO cathode was tested against AC using $Mg(TFSI)_2$ electrolyte salt and a current of 2 mA/g. The capacity delivered during the first charge is around 160 mAh/g, likely due to the higher cut-off potential of +1.2V vs AC. Indeed, if the charge would stop at a cut-off potential of +1.0 V vs AC the same capacity of cell setup nr.2 (around 30 mAh/g) is obtained. The 1st discharge capacity is around 70 mAh/g, and the following cycles show a considerable decrease in capacity already to 40 mAh/g after 5 cycles.

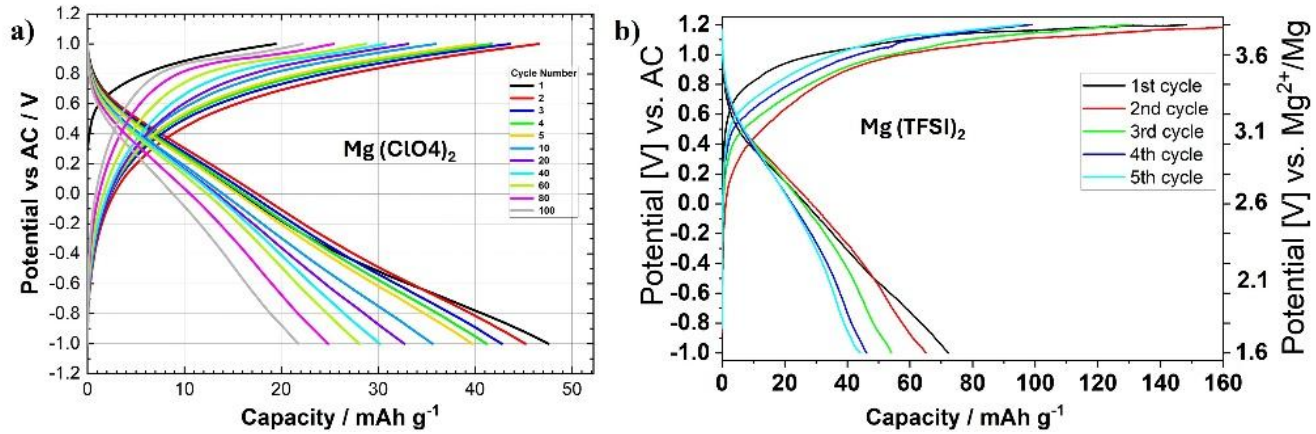

Figure 7. Electrochemical performance of MMO/AC cell at 10 mA/g using (a) $Mg(ClO_4)_2$, (b) Mg $(TFSI)_2$ electrolyte.

Synthesis of the intermetallic Mg-Bi and Mg-Sn alloys:

Since it was not possible to synthesize the intermetallic boundary phases. However, it was decided at the MAGNIFICO kick-off meeting that Mg_2Sn and Mg_3Bi_2 alloys should be used as reference materials. Mg_2Sn and Mg_3Bi_2 alloys were synthesised using a new mechanical alloying method. Mg and Sn or Bi powders were mixed in an appropriate molar ratio, and the mixture was ball-milled for 18 h under an Ar atmosphere using a planetary ball mill. The milling jar (volume, 80 mL) and balls (diameter, 10 mm) were made of stainless steel. The ball to powder ratio was 15:1 and milling speed was 200 rpm. To obtain a homogeneous mixing and to inhibit sticking event of magnesium particles, ¼ volume of milling container was filled with octane. As ball milled MgSn and Mg_3Bi_2 powders were dried at 60 °C under vacuum for 1 day to remove residual octane. The crystal structure of the synthesised Mg_2Sn and Mg_3Bi_2 alloys was identified by XRD analysis, as shown in Figure 8.

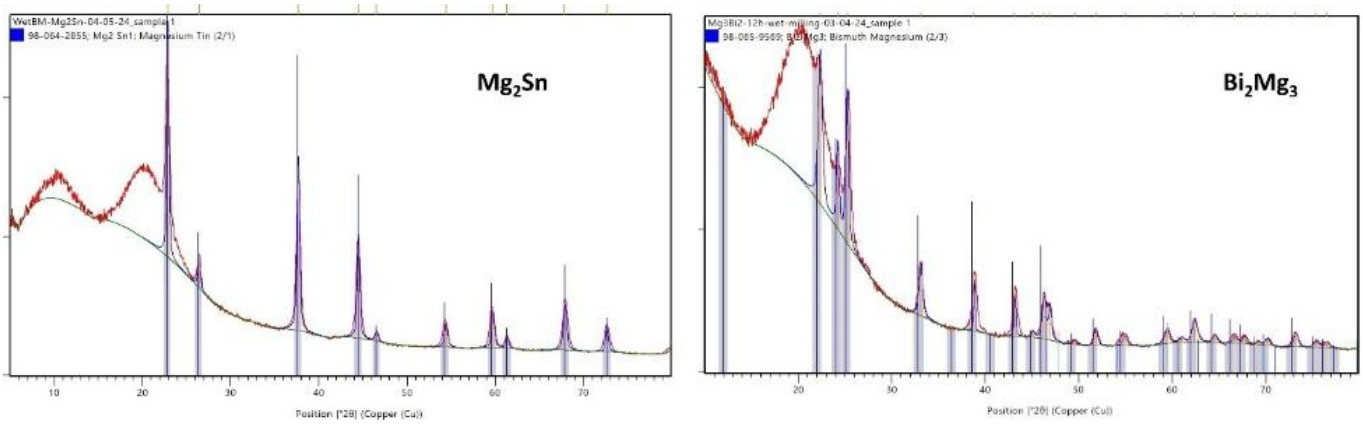

Figure 8. XRD pattern of solvent-based ball-milled synthesised alloys

Density Functional Theory (DFT) analysis of Sn and Bi-based Mg alloy phases

Regarding DFT analysis, three functionals were tested , including PBE[1], PBEsol[2], and SCAN[3], for optimization of Mg, Sn, and Bi metals and well-known stable alloys of Mg-Sn and Mg-Bi. After calculating crystal lattices and formation energies, we chose PBEsol with a 0.02 K-point mesh and a 500 eV cutoff.

The formation energy of different alloys is calculated, as shown in Figure 9. The value of the energy cutoff has no significant effect on formation energy. The results with the 0.02 K-point mesh are close to 0.015, but the difference between 0.03 and 0.015 is substantial. The formation energies of PBEsol are more comparable to SCAN except Mg_3Bi_2. We used PBEsol with a 0.02 K-point mesh and a 500 eV cutoff, based on tests.

Similar to formation energy, results of formation enthalpy at 0 K are also suggest that the Mg_2Sn Fm3m phase is the most stable phase of Mg-Sn alloys. The simulated XRD diffraction patterns of Mg2Sn and Mg3Bi2 matched those of the experimentally synthesised alloys, including those produced by mechanical milling of Mg and Sn or Bi (Figure 8). It can help to verify the synthesized phase.

We performed crystal structure prediction to search for the most stable phases of Mg_2Sn. We have used a force field of Mg-Sn alloy to run molecular dynamics (MD) of Mg_2Sn alloy. A supercell with 96 atoms was chosen in the simulations. The initial structures are generated by slight perturbation of equilibrium structures. Several MD simulations are performed under different temperatures and pressures to sample more configurations by LAMMPS. Then, 200 structures are selected from the trajectories using principal component analysis with the ASAP package. These structures were further calculated using DFT to obtain the Mg2Sn dataset. We used the DP-gen package in conjunction with the DeePMD-kit framework to generate the Mg_3Bi_2 dataset through active learning. A 4×4×2 supercell of Mg_3Bi_2 containing 90 atoms was constructed. An initial dataset was generated by performing perturbations in the cell with lattice scales of 0.97, 1.0, and 1.03. A machine learning potential was fitted to the initial dataset.

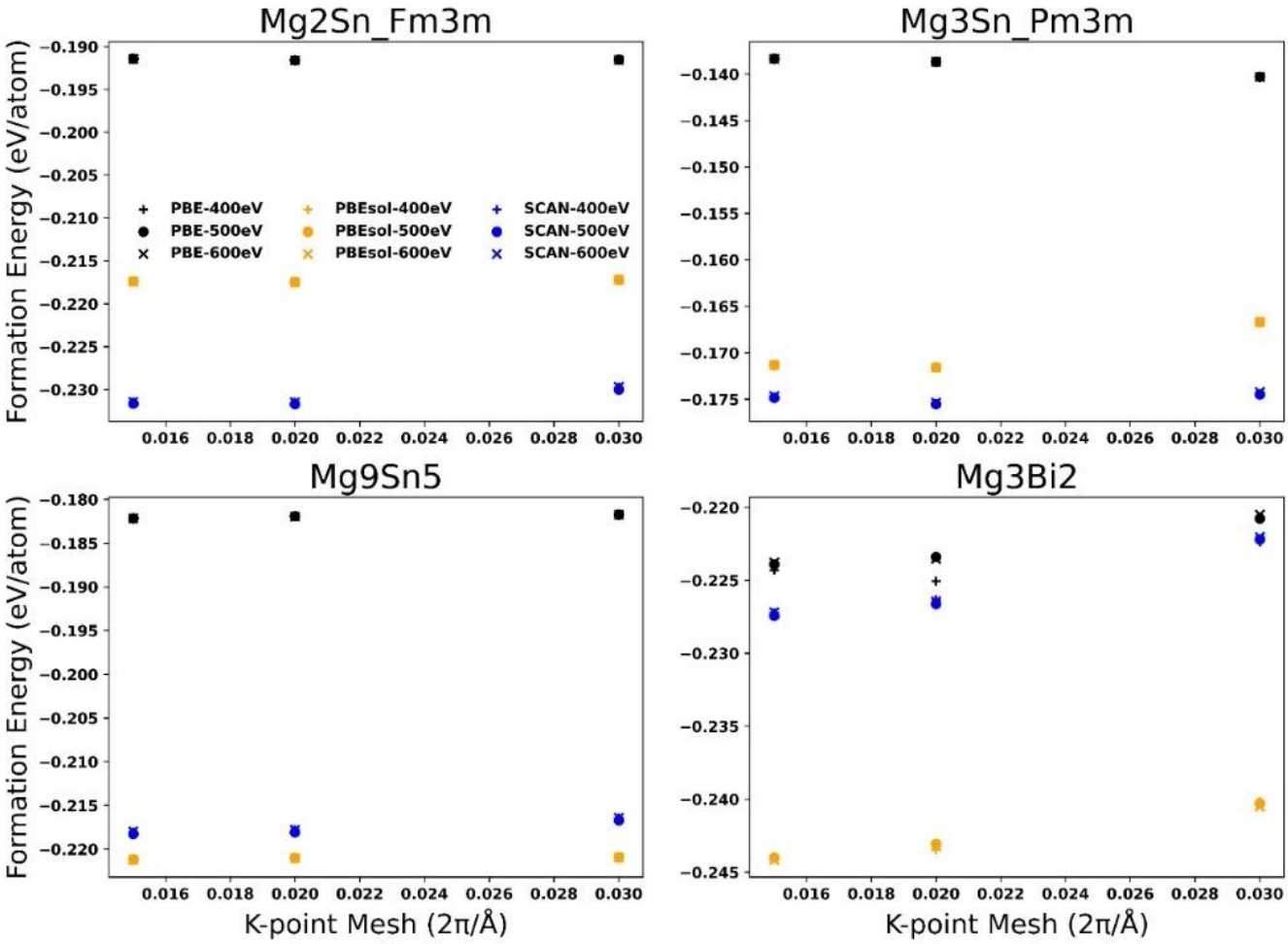

Figure 9. The formation energy of Mg-Sn and Mg-Bi alloys under different calculation parameters.

Machine Learning Potentials (MLP) for Modelling the Coated Mg Powder Anode

Initial machine learning potential calculations (MPLs) for the Mg-Sn and Mg-Bi systems were performed. After obtaining the Mg_2Sn and Mg3Bi2 datasets, we used the DeepMD-kit package to fit a machine learning potential (MLP) with the dataset. The fitting results are shown in Figure 10. True and predicted values present an excellent linear relationship.

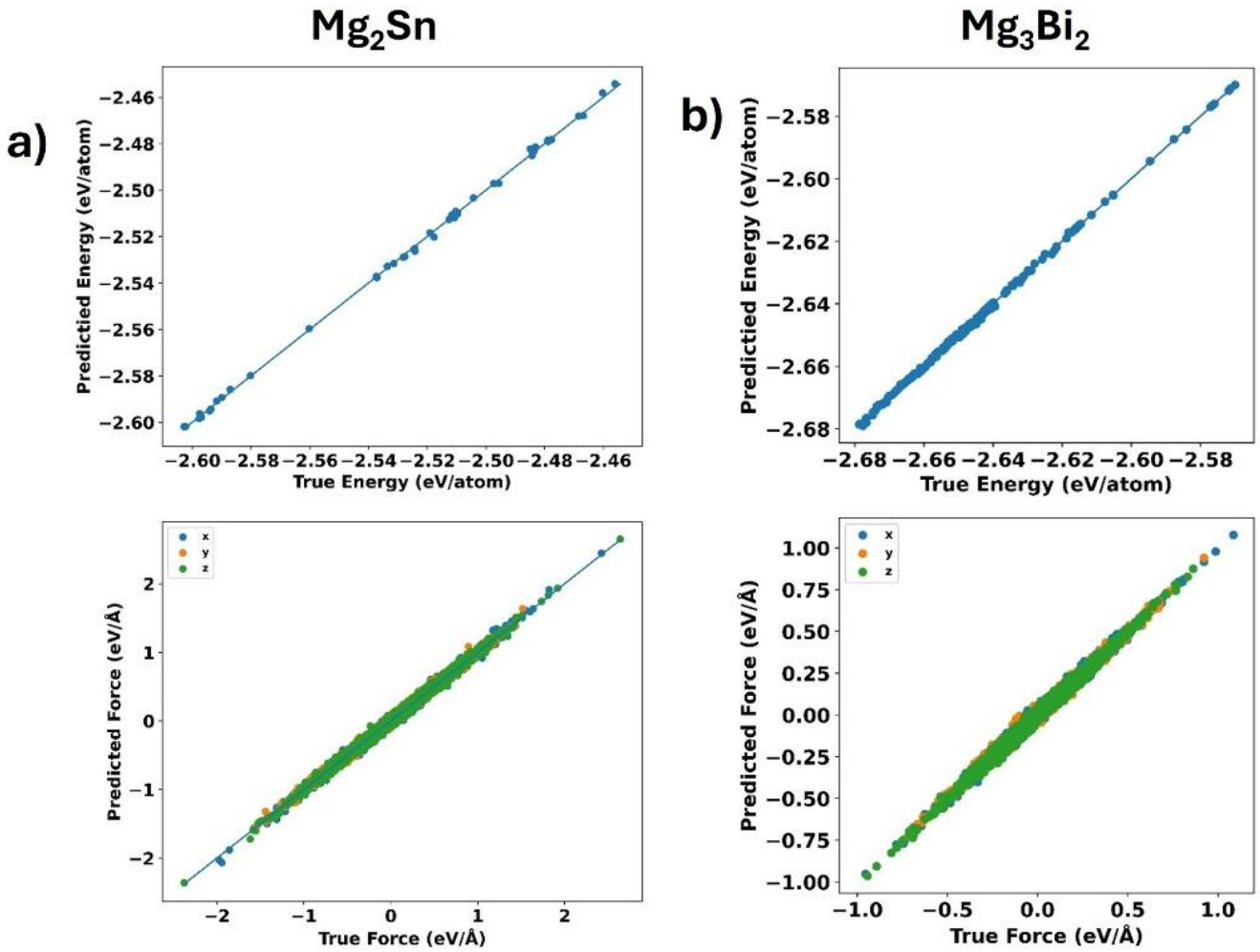

Figure 10. The true energy and force versus the predicted energy and force of the MLP of Mg_2Sn and Mg_3Bi_2.

However, midway through the project, it was realised that a state-of-the-art approach for fitting MLPs to the Mg-Sn and MgBi systems had become outdated. Limitations included insufficient accuracy (three-body interactions only), lack of long-range interactions, and the need for system-specific ("bespoke") models. To address this, we adopted newer methods: long-range MLPs using Latent Ewald Summation (LES), which improve accuracy and transferability, and universal MLPs that work across many materials without custom training. In addition, instead of traditional molecular dynamics for phase behaviour, a new generative modelling approach based on flow matching was developed. This method efficiently samples phase space (including discrete variables like atom types) and can predict material behavior across

temperatures with lower computational cost and better scalability. This new method as well as validations, has been published as a peer-reviewed paper: https://doi.org/10.1021/acs.jctc.5c01248.

Regarding large-scale molecular dynamics simulation, we initially proposed to use molecular dynamics simulations to model nanoparticles. However, recent developments in the machine learning field offers a more efficient alternative. To reduce the cost of predicting the phase behavior of Mg-Sn and Mg-Bi materials, we developed a generative model based on flow matching, a state-of-the-art ML technique, as shown in Figure 11. This approach enables a single model to sample free energy surfaces over a wide temperature range with minimal training overhead, and the model generation is scalable to larger lattice sizes than those in the training set. This framework provides a scalable and computationally efficient solution for discrete coordinate systems and can be extended to sample the alchemical degrees of freedom in crystalline compounds.

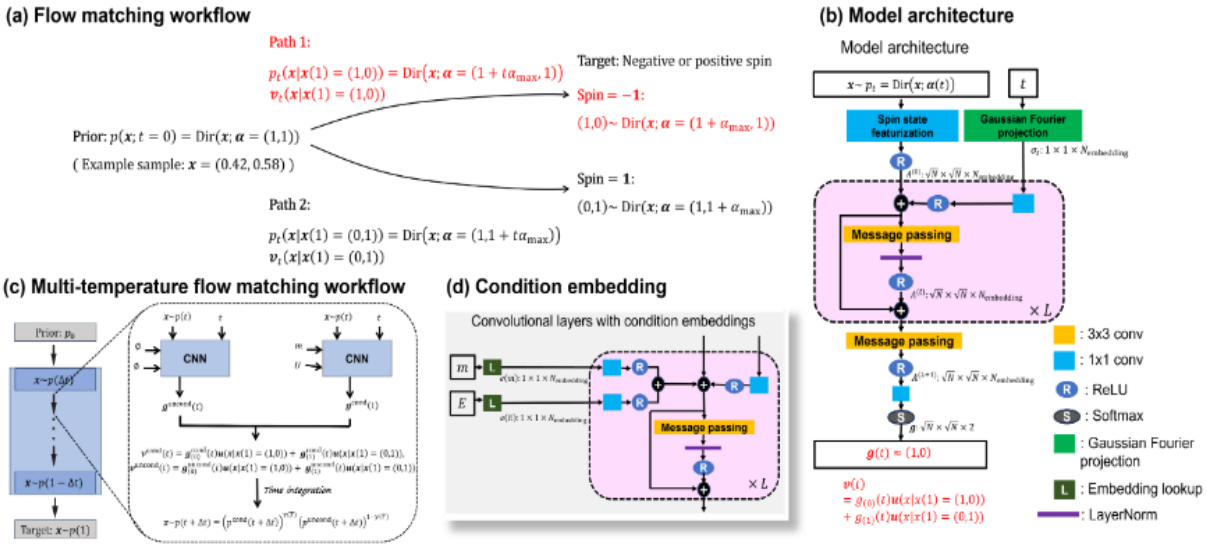

Figure 11. A schematic of the flow matching method for alchemical sampling.

4 Ergebnisse und Schlussfolgerungen

In sum, the MAGNIFICO project successfully developed a scalable wet-chemical process for protecting Mg powder anodes with uniform Sn-based coatings, enabling stable and reversible Mg plating/stripping in conventional $Mg(TFSI)_2$ electrolytes. This protection suppressed passivation and electrolyte decomposition while maintaining efficient Mg^{2+} diffusion, resulting in high-capacity full cells (≈70–80 mAh g^{-1}). Additionally, etched Mg powder electrodes based full cells show high capacity, superior rate capability, and the first demonstration in pouch-cell format using APC electrolyte. Complementary DFT, alloy synthesis, and advanced machine-learning potentials (including long-range and generative flow-matching approaches) provided deeper insights into phase stability and accelerated materials discovery.

5 Ausblick und Empfehlungen

These results pave the way for safer, more sustainable, and cost-effective high-voltage magnesium-ion batteries that minimise critical raw materials, offering a viable pathway toward next-generation energy storage with improved energy density, cycle life, and environmental benefits for large-scale applications. Further study is already being undertaken in EU-funded projects such as HighMag, see https://highmag-project.eu , also led by AIT's battery group.

6 Literaturverzeichnis

Ping Tuo, Zezhu Zeng, Jiale Chen, Bingqing Cheng; Scalable Multitemperature Free Energy Sampling of Classical Ising Spin States. *J. Chem. Theory Comput.* 25 November 2025; 21 (22): 11427–11435. https://doi.org/10.1021/acs.jctc.5c01248

7 Kontaktdaten

Dr. Irshad MOHAMMAD
AIT Austrian Institute of Technology GmbH
Giefinggasse 2, 1210 Wien, Tel 050550, www.ait.ac.at, MAGNIFICO Development of a protective inorganic interface for using metallic Mg anodes - AIT Austrian Institute Of Technology

Project partner:
ISTA Institute of Science and Technology Austria